The Pennsylvania State University
Institute for Science and Engineering
APPLIED RESEARCH LABORATORY
Post Office Box 30
State College, Pa. 16801

NAVY DEPARTMENT

NAVAL SEA SYSTEMS COMMAND

CAVITATION RESULTS FOR A SECONDARY FLOW GENERATED

TRAILING VORTEX

M. L. Billet

Techanical Memorandum
File No. TM 76-234
24 August 1976
Contract No. N00017-73-C-1418

Copy No. _____

TM-76-234

The Pennsylvania State University
APPLIED RESEARCH LABORATORY
Post Office Box 30
State College, PA 16801

SECURITY CLASSIFICATION OF THIS PAGE (When Data Entered)

REPORT DOCUMENTATION PAGE		READ INSTRUCTIONS BEFORE COMPLETING FORM
1. REPORT NUMBER TM 76-234	2. GOVT ACCESSION NO.	3. RECIPIENT'S CATALOG NUMBER
4. TITLE (and Subtitle) CAVITATION RESULTS FOR A SECONDARY FLOW GENERATED TRAILING VORTEX		5. TYPE OF REPORT & PERIOD COVERED
		6. PERFORMING ORG. REPORT NUMBER
7. AUTHOR(s) M. L. Billet		8. CONTRACT OR GRANT NUMBER(s) N00017-73-C-1418
9. PERFORMING ORGANIZATION NAME AND ADDRESS Applied Research Laboratory P. O. Box 30 State College, PA 16801		10. PROGRAM ELEMENT, PROJECT, TASK AREA & WORK UNIT NUMBERS
11. CONTROLLING OFFICE NAME AND ADDRESS Naval Sea Systems Command Washington, DC 20362		12. REPORT DATE 24 August 1976
		13. NUMBER OF PAGES 22
14. MONITORING AGENCY NAME & ADDRESS(if different from Controlling Office)		15. SECURITY CLASS. (of this report) UNCLASSIFIED
		15a. DECLASSIFICATION/DOWNGRADING SCHEDULE

16. DISTRIBUTION STATEMENT (of this Report)

Approved for public release. Distribution unlimited.
Per NAVSEA –

17. DISTRIBUTION STATEMENT (of the abstract entered in Block 20, if different from Report)

18. SUPPLEMENTARY NOTES

19. KEY WORDS (Continue on reverse side if necessary and identify by block number)

Boundary Layer   Vorticity
Rotor   Flow Coefficient
Water Tunnel
Cavitation

20. ABSTRACT (Continue on reverse side if necessary and identify by block number)

Limited cavitation numbers were obtained for a trailing vortex generated by the interaction of a boundary layer and a rotor when the boundary layer thickness is the same order of magnitude as the rotor radius. The results were obtained for various boundary layer profiles and velocities in the 48-inch diameter water tunnel.

DD FORM 1473 EDITION OF 1 NOV 65 IS OBSOLETE
1 JAN 73

SECURITY CLASSIFICATION OF THIS PAGE (When Data Entered)

From: M. L. Billet

Subject: *Cavitation Results for a Secondary Flow Generated Trailing Vortex*

References: See page 13.

Abstract: Limited cavitation numbers were obtained for a trailing vortex
generated by the interaction of a boundary layer and a
rotor when the boundary layer thickness is the same order
of magnitude as the rotor radius. The results were
obtained for various boundary layer profiles and velocities
in the 48-inch diameter water tunnel.

24 August 1976
MLB:jep

Table of Contents

List of Figures

List of Tables

Nomenclature

C_p -   characteristic pressure coefficient

$C_{p_{min}}$ -   minimum pressure coefficient

P_G -   pressure typical of the noncondensable gas in a bubble

$P_{G_{max}}$ -   maximum gas pressure in a bubble

P_{min} -   minimum pressure

P_v -   vapor pressure based on liquid temperature

P_∞ -   static pressure of infinity

P_{∞_ℓ} -   static pressure at infinity for limited cavitation

U_{TIP} -   rotor tip velocity

V_∞ -   velocity at infinity

α -   dissolved gas content of the liquid

β -   Henry's Law constant

ϕ -   flow coefficient

σ -   cavitation number

σ_d -   desinent cavitation number

σ_ℓ -   limited cavitation number

ρ -   mass density of the liquid

INTRODUCTION

Secondary flows generate additional streamwise vorticity when a boundary layer flow is turned by a rotor. The apparent effect of this additional vorticity is evidenced by a cavitating trailing vortex. The cavitation number of this vortex which exists in the complicated flow downstream of the rotor is a measure of the amount of streamwise vorticity near the wall of the rotor. In most cases, the critical cavitation numbers typical this trailing vortex system are often higher than those associated with any other type of cavitation.

Vortex cavitation is one of the least understood forms of cavitation. It is felt that this lack of understanding is due to an inadequate knowledge of the flow field and the effects of noncondensable gases. As an example, the structure of the trailing vortex created in the passage of a rotor is influenced very significantly by variations of the incoming boundary layer to the rotor. Also, vortex flows tend to be good collectors of gas bubbles which can cause nonvaporous cavitation. The cavitation numbers associated with limited nonvaporous cavitation are often considerably higher than those for limited vaporous cavitation.

In this investigation, experimentally determined cavitation numbers for the trailing vortex system were obtained for various incoming boundary layer profiles and flow coefficients. Also, the effect of air content on the cavitation number was determined.

BACKGROUND

Cavitation flows are delineated by the cavitation number, σ, defined as

$$\sigma \equiv \frac{P_\infty - P_v}{1/2\rho \, V_\infty^2} \tag{1}$$

where P_∞, V_∞, P_V and ρ are the pressure at infinity, the velocity at infinity, the vapor pressure, and the mass density of the liquid, respectively. The fluid properties correspond to the bulk temperature of the liquid.

The flow regime of particular concern is limited cavitation, i.e. the extent of cavitation is minimized. The problem of limited cavitation has been reviewed in recent years by Holl [1][*] and Holl, Arndt, and Billet [2].

The particular value of σ corresponding to limited cavitation is the limited cavitation number σ_ℓ, or critical cavitation number given by

$$\sigma_\ell = \frac{P_{\infty_\ell} - P_v}{1/2\rho\, V_\infty^2} \quad . \tag{2}$$

In this investigation, σ_ℓ is determined by a desinence test so that

$$\sigma_\ell = \sigma_d \tag{3}$$

where σ_d is the desinent cavitation number [3]. The limited cavitation number can also be determined by an inception test, provided hysteresis effects are not involved [4].

There are two general types of limited cavitation, namely vaporous and nonvaporous cavitation. To visualize the various types of limited cavitation, it is useful to imagine that one is observing the growth of a single bubble as the pressure is suddenly reduced. Vaporour cavitation

----

[*] Numbers in brackets refer to documents given in the list of references.

occurs at pressures less than vapor pressure and is characterized by
the explosive growth of a bubble due to the rapid conversion of liquid
to vapor at the bubble wall. There are two types of nonvaporous
cavitation, namely pseudo and gaseous cavitation. Pseudo cavitation
occurs when a bubble merely expands due to a reduction in pressure
with the mass of gas in the bubble essentially remaining constant.
Gaseous cavitation occurs when a bubble grows in an oversaturated liquid
due to the transport of gas across the interface. In contrast to
vaporous cavitation, nonvaporous cavitation can occur at pressures
greater than vapor pressure.

Of particular importance in the study of limited cavitation is the
minimum pressure coefficient, $C_{p_{min}}$, given by

$$C_{p_{min}} \equiv \frac{P_\infty - P_{min}}{1/2\rho\ V_\infty^2} \tag{4}$$

where p_{min} is the minimum pressure.

In general, results indicate for vaporous limited cavitation that

$$\sigma_\ell \leq C_{p_{min}} \tag{5}$$

In principle, nonvaporous cavitation can occur below or above vapor
pressure [1]. However, from a practical point of view, it is the latter
type which is the most interesting because of the large values of
cavitation numbers which are often typical of these cases [1]. Thus,
for nonvaporous limited cavitation occurring at pressures above vapor
pressure

$$\sigma_\ell > C_{P_{min}} \quad . \tag{6}$$

In 1960, Holl [3] employing an equilibrium theory which ignored surface tension effects predicted for nonvaporous cavitation that

$$\sigma_\ell = C_p + \frac{P_G}{1/2\rho \, V_\infty^2} \quad , \tag{7}$$

where C_p is a characteristic pressure coefficient, and P_G is a pressure typical of the noncondensable gas in the bubbles. Holl indicated that there was an upper limit to the gas pressure, namely the equilibrium value given by Henry's Law which may be expressed in the form

$$P_{G_{max}} = \alpha\beta \quad , \tag{8}$$

where α is the dissolved gas content and β the Henry's Law constant.

Several general implications come from Equation (7). Firstly, the equation predicts that σ_ℓ is a monotonically decreasing function of velocity for constant values of P_G and C_p. Secondly, the equation predicts excessively large values of σ_ℓ at low velocities. These results suggest that, if one is to avoid confusing nonvaporous for vaporous cavitation, it is advisable to conduct tests at high velocities. The aforementioned tendency for σ_ℓ to decrease with velocity for nonvaporous cavitation is characteristic of data reported by several authors, namely, Hammitt et al. [5], Lindgren and Johnson [6], McCormick [7], and Ripken and Killen [8].

Thus, it is very important to understand the differences between vaporous and nonvaporous cavitation in order to interpret test data. It

is also apparent in view of Equations (5) and (6) that it is very important to know C_p in order to differentiate between various flow states. However, in many flows C_p data are not available so that other means for differentiating between flow states, such as noise spectra, are needed.

DESCRIPTION OF THE EXPERIMENTS

The experiments were conducted with water near room temperature in the 48-inch diameter tunnel located in the Garfield Thomas Water Tunnel Building of the Applied Research Laboratory at The Pennsylvania State University. In all cases, desinent cavitation was employed as the experimental measure of limited cavitation. Limited cavitation in the trailing vortex system occurred at the cone tip which was behind the rotor located at the end of the axisymmetric forebody. Also, the occurrence of the cavitation was very sporadic.

The air content was approximately 3.1 ppm for all of the experiments except for one experiment which had a range of air contents. The air content of 3.1 ppm was chosen because gas effects are reduced and the relative saturation level was always much less than unity.

Desinent cavitation number data were obtained for different incoming velocity profiles to the rotor. The incoming velocity profile was varied by changes in the configuration of the axisymmetric forebody. Results were obtained with/without upstream appendages, with/without a screen on the nose of the axisymmetric forebody, and on/off design rotor flow coefficients. In addition, two different tip designs were employed behind the rotor. These basic flows are described in Table 1 and the tip designs are sketched in Figure 1.

DISCUSSION OF RESULTS

The desinent cavitation number data are shown in Figures 2-8 where the effects of the following factors are displayed:

Figure 2 - Effect of Air Content

Figure 3 - Effect of Tip Design

Figure 4 - Effect of Flow Coefficient

Figure 5 - Effect of Upstream Appendages

Figure 6 - Effect of Upstream Appendages and Screens

Figure 7 - Effect of Screen and Flow Coefficient with Appendages

Figure 8 - Effect of Screens and Flow Coefficient without Appendages

Thus, Figures 2-8 display the effects of air content, tip design, flow coefficient, upstream appendages, and upstream screens on the desinent cavitation number.

In general, an increase in gas content, the addition of upstream appendages, or a 10% decrease in flow coefficient cause the cavitation number to increase. In contrast to these results, the addition of upstream screens or a 10% increase in flow coefficient cause the cavitation number to decrease.

Data in Figure 4 shows that a decrease in the flow coefficient by 10% causes a dramatic increase in the cavitation number, whereas a 10% increase in the flow coefficient causes the opposite trend. The cavitation number at the design flow coefficient increases slowly with velocity, whereas at 10% below the design flow coefficient, it increases rapidly with velocity. In contrast to these trends, at a flow coefficient 10% above the design value, the cavitation number decreases with velocity.

The effect of upstream appendages is displayed by the data in Figures
5 and 6, where the appendages are in the form of four struts upstream of
the rotor. It is seen that the addition of the appendages increases
the cavitation number by 50 to 70%.

The effect of tip design is shown by the data in Figure 3. The data
indicates that the conical tip causes cavitation numbers which increase
with velocity and range between 4.5 and 5.1. In contrast to this trend,
the truncated conical tip causes much higher cavitation numbers which
tent to decrease with an increase in velocity. This velocity trend is in
agreement with the equilibrium theory discussed in the background
information. Assuming that C_{Pmin} and P_G are essentially constant, then
Equation (7) can be expressed as

$$\sigma_d = \text{constant} + \frac{\text{constant}}{V_\infty^2} \quad . \tag{9}$$

The data for the truncated cone tip approximate this trend. Apparently,
the separated flow increases the residence time of bubbles in the low
pressure region which accentuates the gas effects predicted by the
equilibrium theory.

The data in Figure 2 also show gas effects on the cavitation number.
As the gas content increases, the cavitation number tends to increases.

SUMMARY

Cavitation numbers for trailing vortex cavitation from a rotor
vary significantly with upstream configurations. Variations in the
shape of the incoming boundary layer influences the loading on the rotor
near the hub. This causes variations in the amount of inlet vorticity to
the rotor passage and variations in the amount of secondary vorticity
generated in the blade passage. Small changes in the profile result in

a large increase in the cavitation number as shown by the addition of

upstream appendages. A 10% decrease in the flow coefficient causes an

increase in σ whereas a 10% increase in the flow coefficient yields the

opposite trend. The cavitation number is sensitive to air content

effects, particularly for the truncated conical tip design.

REFERENCES

1. J. W. Holl, "Limited Cavitation," Proceedings of the Symposium on Cavitation State of Knowledge, ASME, June 1969, pp. 26-63.

2. J. W. Holl, R. E. A. Arndt, and M. L. Billet, "Limited Cavitation and the Related Scale Effects Problem," Proc. Second Int. JSME Symp. on Fluid Machinery and Fluidics, Tokyo, September 1972, pp. 303-314.

3. J. W. Holl, "An Effect of Air Content on the Occurrence of Cavitation," Journal of Basic Engineering, Trans. ASME, Series D, Vol. 82, 1960, pp. 941-946.

4. J. W. Holl and A. L. Treaster, "Cavitation Hysteresis," Journal of Basic Engineering, Trans. ASME, Series D, March 1966, pp. 199-212.

5. F. G. Hammitt, J. F. Lafferty, D. M. Ericson, and M. J. Robinson, "Gas Content, Size, Temperature and Velocity Effects on Cavitation Inception in a Venturi," ASME Paper 67 WA/FE 22, 1967.

6. H. Lindgren and C. A. Johnson, "Cavitation Inception on Head Forms - ITTC Comparative Experiments," Report No. 58, Swedish State Ship-building Experimental Tank, 1966.

7. B. W. McCormick, "On Cavitation Produced by a Vortex Trailing from a Lifting Surface," Journal of Basic Engineering, Trans. ASME, September 1962, pp. 369-379.

8. J. F. Ripken and J. M. Killen, "Gas Bubbles: Their Occurrence, Measurements, and Influence in Cavitation Testing," Proceedings of IAHR Symposium, Sendai, Japan, 1962, pp. 37-57.

TABLE 1

Basic Flow Configurations

Number	Upstream Appendages**	Upstream Screen	Rotor Flow Coefficient (ϕ)	Tip Design
1	No	No	$\phi = \phi_d$*	Conical
2	No	No	$\phi = 0.9\phi_d$	Conical
3	No	Yes	$\phi = \phi_d$	Conical
4	Yes	No	$\phi = \phi_d$	Conical
5	Yes	No	$\phi = 1.1\phi_d$	Conical
6	Yes	No	$\phi = 0.9\phi_d$	Conical
7	Yes	Yes	$\phi = \phi_d$	Conical
8	Yes	Yes	$\phi = 0.9\phi_d$	Conical
9	No	Yes	$\phi = 0.9\phi_d$	Conical
10	Yes	No	$\phi = \phi_d$	Truncated – Conical

* ϕ_d = design flow coefficient $\equiv V_\infty/U_{TIP}$

** The upstream appendages consisted of four struts placed at the 0°, 90°, 180°, 270° points on the axisymmetric test body.

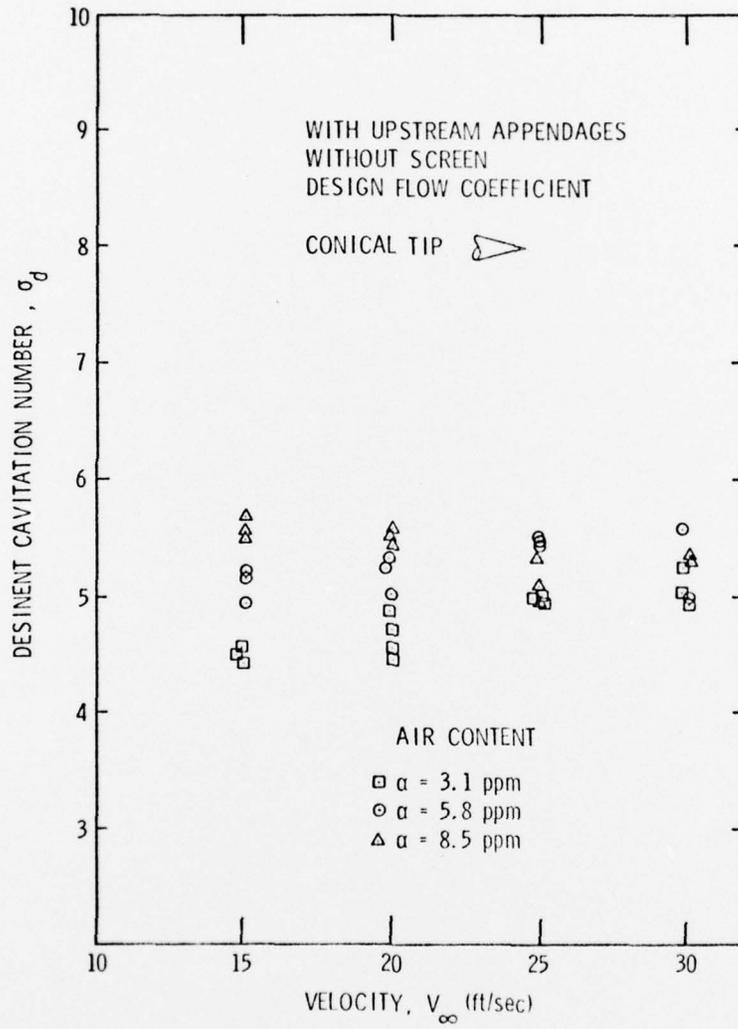TRUNCATED CONICAL TIP
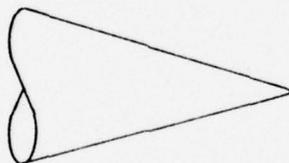
CONICAL TIP

Figure 1 - Tip Designs

Figure 2 - Cavitation Data - Effect of Air Content
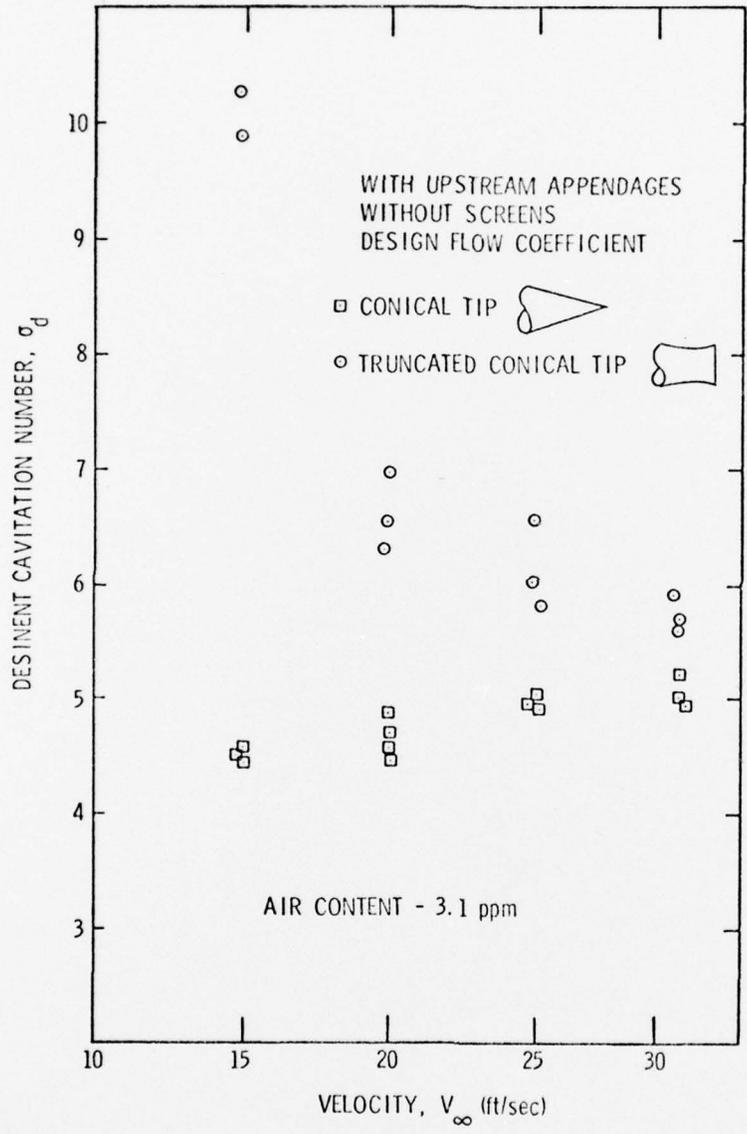(Basic Flow #4)

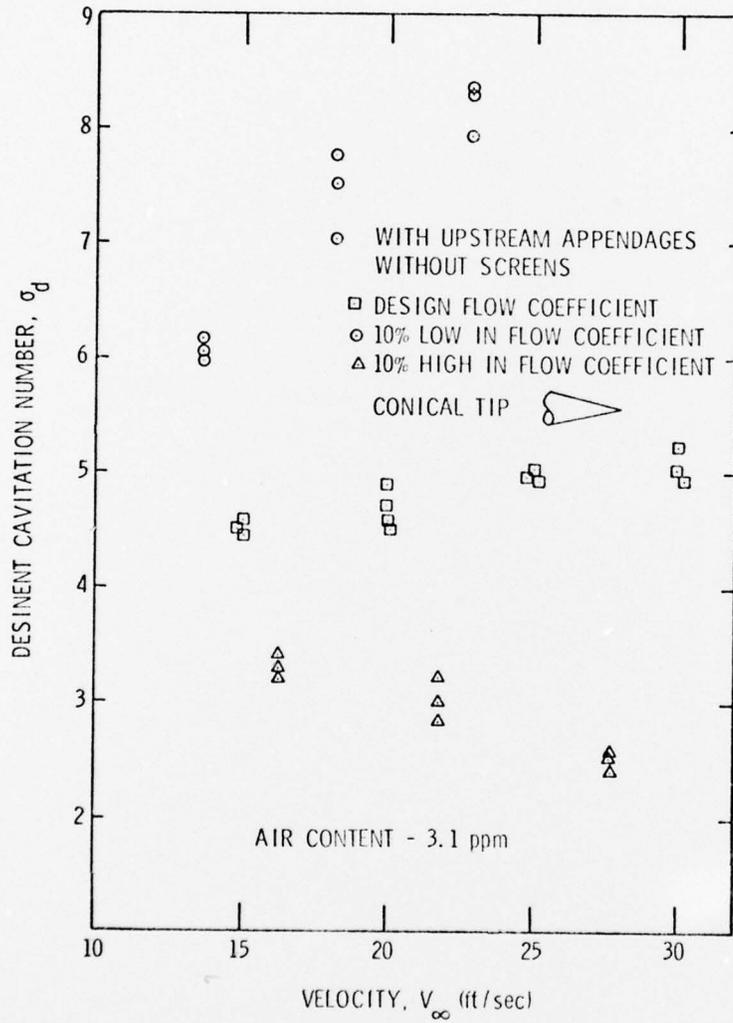Figure 3 – Cavitation Data – Effect of Tip Design
(Basic Flows #4, #10)

Figure 4 - Cavitation Data - Effect of Flow Coefficient
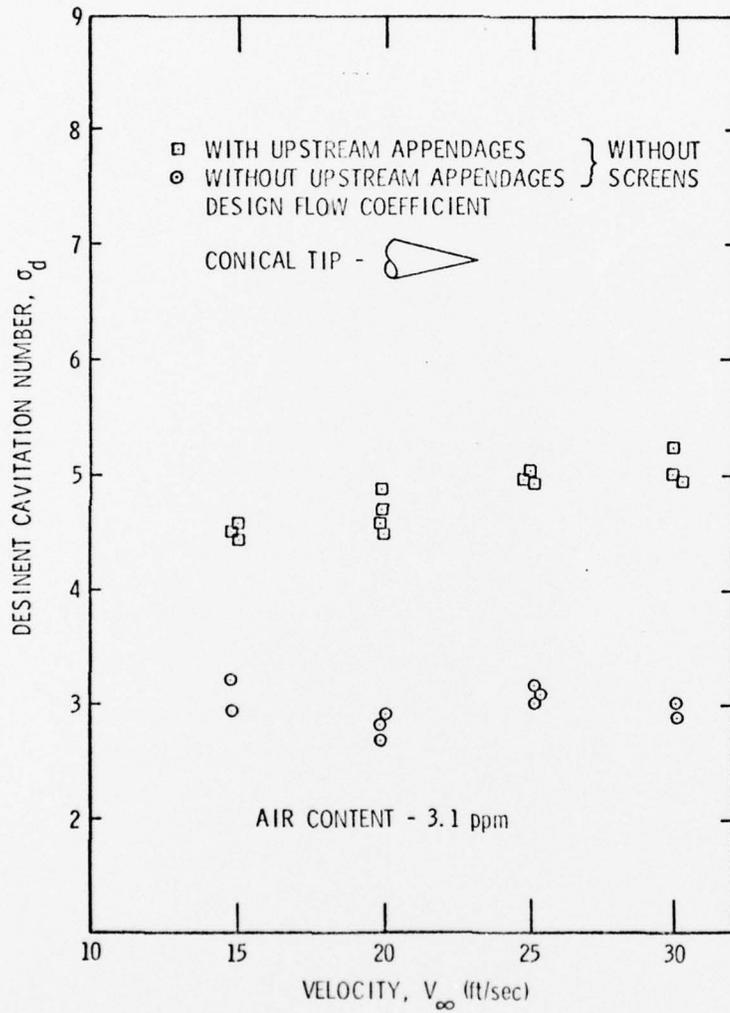(Basic Flows #4, #5, #6)

Figure 5 – Cavitation Data- Effect of Appendages
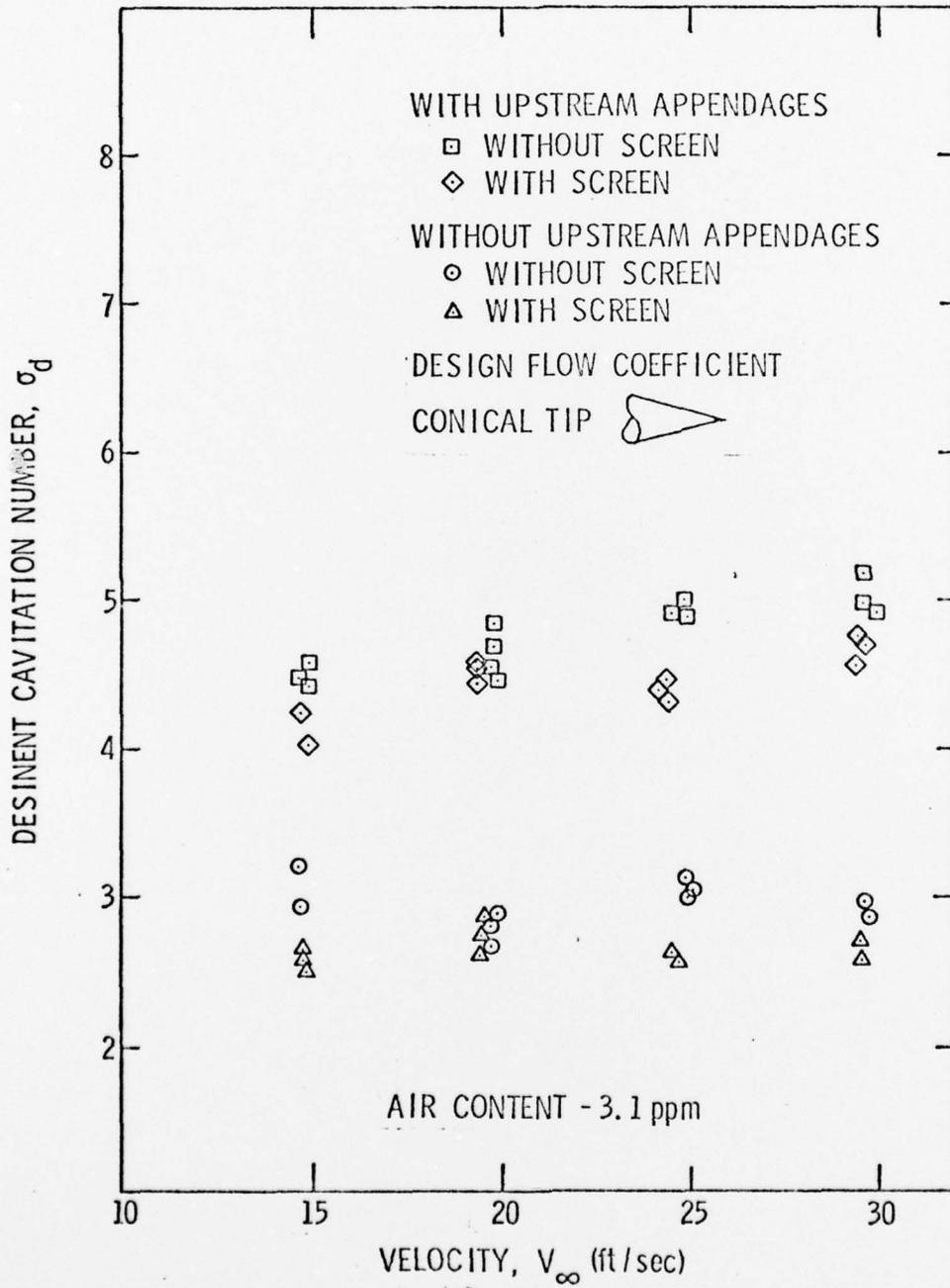(Basic Flows #1, #4)

Figure 6 – Cavitation Data – Effect of Appendages and
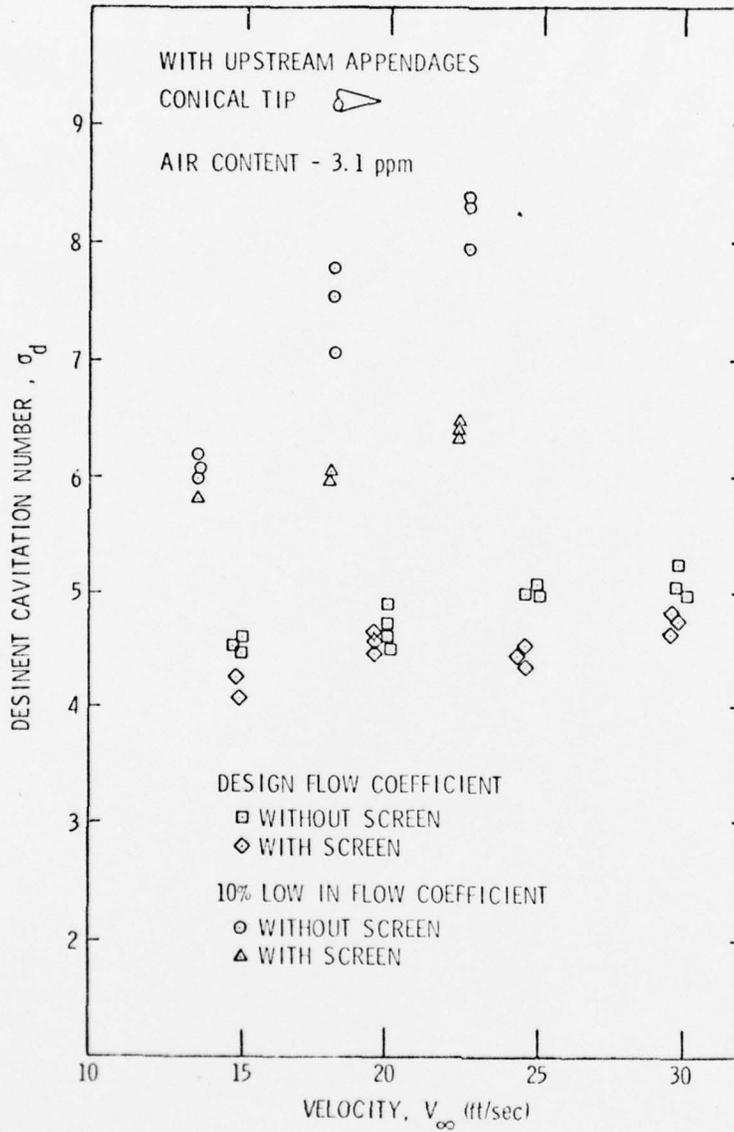Screen (Basic Flows #1, #3, #4, #7)

Figure 7 - Cavitation Data - Effect of Screen and Flow
    Coefficient with Appendages (Basic Flows #4,
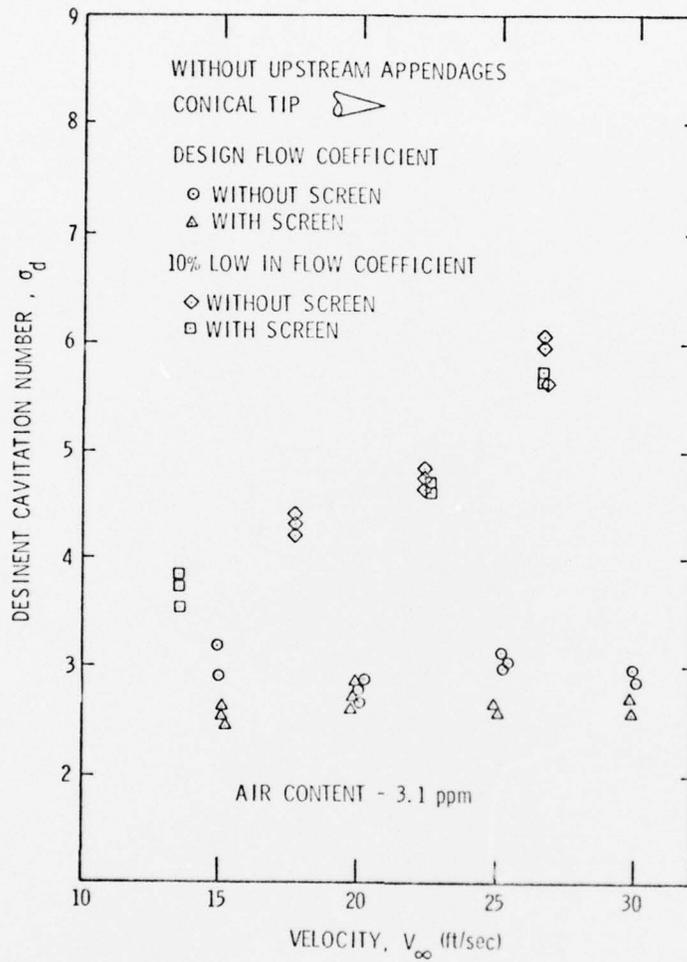   #6, #7, #8)

Figure 8 – Cavitation Data – Effect of Screen and Flow
Coefficient Without Appendages (Basic Flows
#1, #2, #9)